

## Determination of the lattice relaxation at the Yb(111) surface using chemical-shift photoelectron diffraction

M. E. Dávila,<sup>1,2</sup> S. L. Molodtsov,<sup>3</sup> M. C. Asensio,<sup>1,2</sup> and C. Laubschat<sup>3</sup>

<sup>1</sup>*Instituto de Ciencias de Materiales de Madrid (CSIC), 28049 Cantoblanco, Madrid, Spain*

<sup>2</sup>*LURE, Bâtiment 209D, Université de Paris-Sud, Boîte Postale 34, 91898 Orsay, France*

<sup>3</sup>*Institut für Oberflächenphysik und Mikrostrukturphysik, TU Dresden, D-01062 Dresden, Germany*

(Received 27 December 1999)

A quantitative analysis of the surface relaxation of thick Yb(111) single-crystal films grown on W(110) has been performed by photoelectron diffraction technique using high-energy resolution photoemission spectra of the surface core-level shift of Yb 4*f*. Our results demonstrate that Yb grows epitaxially in a fcc structure without surface reconstruction. The surface atoms present an inward relaxation of the first and second layers by  $(3.6 \pm 0.3)\%$  and  $(1.9 \pm 0.2)\%$  of the bulk interlayer spacing, respectively. The appearance of the *d*-like surface-state at Yb(111) is assumed to be responsible for the inward surface relaxation.

Changes in the electronic and crystallographic properties at the surfaces are by now well-known phenomena that become particularly interesting when the chemical and magnetic properties of the materials are affected.<sup>1,2</sup> This is the case in rare-earth (RE) solids where both 4*f* occupation and magnetic order depends critically on the electronic and structural environment. Many RE compounds reveal surface valence transitions characterized by an enhancement of the 4*f* occupation at the surface.<sup>3</sup> Among the pure RE metals this phenomenon occurs for Ce, Sm, and Tm, where the valence and magnetic properties of the surface atoms change dramatically. Other RE metals like Gd, which do not change the valence of the atoms at the upper surface layers, show an enhancement of their surface magnetic ordering temperature that may be related to structural surface relaxations or to the appearance of electronic surface states.<sup>4-10</sup>

Calculations for the close-packed Gd(0001) surface predict an antiferromagnetic coupling of the outermost atomic surface layer with respect to the bulk, which is accompanied by (i) an outward relaxation of the surface layer by 5% of the lattice constant and (ii) a weakly dispersive antibonding surface state of *d* symmetry.<sup>2</sup> In fact, a *d*-like surface state has been observed experimentally, which is pinned to the Fermi energy and extended over almost the whole surface of the Brillouin zone. The magnetic order of the outermost atomic surface layer, however, is found to be ferromagnetic in contrast to the antiferromagnetic behavior predicted by the theory.<sup>9</sup> Outward surface relaxations as well as *d*-like surface states were also predicted for the closed-packed surfaces of other RE's. For Yb metal, surface states are expected to be unoccupied in the paramagnetic phase. Photoemission studies, however, reveal the existence of occupied surface states at the close-packed surfaces of almost all trivalent RE metals independent on their magnetic order.<sup>11-13</sup> In particular, for the fcc close-packed surface of divalent Yb metal, a surface state has been observed.<sup>14,15</sup>

As may be concluded from these examples, the electronic properties at the surface of rare-earth solids are presently not well understood. Occupation of the weakly dispersive surface states demands large redistribution of charge at the surface, which is obviously not reproduced by the model calcu-

lations. On the other hand, such a redistribution of charge will influence the bonding properties at the surface and may probably affect the lattice relaxation. In this case, strong effects will be expected for the surface divalent Yb metal where the change of the electronic properties is particularly large: in the bulk, the electronic structure is similar to the one of heavy lanthanide earth metals characterized by an almost occupied *s* band with weak 5*d* admixtures in the region close to the Fermi energy. From this scenario a narrowing of the *d* bands caused by the reduced coordination at the surface should result in dehybridization, which may lead to an outward relaxation of the outermost atomic layer as in the case of divalent Be and Mg metal.<sup>16-18</sup> However, the existence of a *d*-like surface state may change this behavior since the electronic spill-out related with such a state as well as its possible contribution to bonding may favor inward relaxation.

In the present communication we report on an experimental determination of the surface lattice relaxation of Yb(111) by means of photoelectron diffraction (PED). In particular, we use the surface core-level shift (SCS) in order to extract quantitative information of the bulk and surface lattice relaxation. Yb metal is ideally suited for this type of experiment since (i) the SCS is large [ $0.45 \pm 0.03$  eV for the closed-packed Yb(111) surface] and allows for proper discrimination of bulk and surface signals even at low spectral resolution. (ii) Due to its 4*f* (Ref. 14) ground-state configuration, the 4*f* emission of divalent Yb consists of a simple 4*f* (Ref. 13) final-state doublet that is not affected by resonant cross-section variations like the 4*f* emissions of other RE's. (iii) The chemical reactivity of Yb metal is relatively weak allowing for large sampling times as necessary for PED experiments. Moreover, possible contaminants like C and O lead usually to the formation of trivalent compounds, which may easily be identified by their characteristic chemical shift by 4 eV to higher binding energies (BE's) of the 4*f* core level. Our results reveal an inward relaxation of the first two layers by  $(3.6 \pm 0.3)\%$  and  $(1.9 \pm 0.2)\%$  of the bulk interlayer spacing, respectively, i.e.,  $(1.8 \pm 0.3)\%$  and  $(1.1 \pm 0.3)\%$  in terms of the bulk lattice constant. This finding differs from the

experimental results on divalent metals like Be and Mg where an outward relaxation has been observed.<sup>16–18</sup> Thus, an intimate relation between the lattice relaxation and the appearance of the *d*-like surface state may be expected.<sup>14</sup>

In the present experiment scanned energy PED beams have been taken for surface and bulk components of the Yb 4*f* (Ref. 13) emission at several constant emission angles in the photon energy range from 140 to 260 eV. Additionally, polar scans have been performed at a fixed “surface sensitive” photon energy of 150 eV. In this way two traditional independent modes of PED (energy and angular scans) were combined in order to determine surface lattice relaxations with accuracy of 0.03 Å. The PED experiments were performed at the Super-ACO storage ring at (L.U.R.E./Orsay) using radiation from the SU7 beamline. PE spectra were taken with a routable hemispherical electron energy analyzer (ARIES-VSW) tuned to an acceptance angle of 1°. PED energy scans were taken at different geometries tuning the photon energy from 140 to 260 eV in steps of 2 eV. Additionally, a series of polar-angle scans were recorded along the high symmetry azimuthal directions varying the polar ( $\theta$ ) angle from 0° to 60° off normal. Variations of the relative intensities of bulk and surface emissions were analyzed by consistent least-squares fitting of the whole set of experimental data. Well-ordered Yb(111) surfaces were prepared by growing well-ordered epitaxial Yb films on a W(110) substrate. The clean W(110) surface was obtained after successive cycles of annealing at 1300 °C in oxygen atmosphere that ensured a sharp (1×1) hexagonal low-energy electron diffraction (LEED) pattern. Thick Yb layers (80–100 Å), monitored by a quartz microbalance, were deposited onto the tungsten substrate by thermal evaporation from Yb metal drops molten on tantalum straps. “As-grown” films revealed a rather diffuse LEED pattern pointing to weak structural order at the surface. Annealing at 180 °C led to a sharp hexagonal LEED pattern characteristic for the close-packed Yb (111) surface. The quality of the Yb film was further checked by valence-band PE spectra at 150 eV photon energy. A typical spectrum is displayed in Fig. 1, where two well-resolved spin-orbit split doublets corresponding to 4*f* emissions from bulk and surface, respectively, can be identified separated by a SCS of  $0.47 \pm 0.02$  eV that is characteristic of a very clean and highly coordinated surface.

The PE spectra of the Yb 4*f* (Ref. 13) final states were approximated by two pairs of Lorentians (Fig. 1) accounting for bulk (full line) and surface (broken line) components. The weak contribution of the 6*s* valence band was described by a steplike function with a cutoff at  $E_F$ . To account for secondary electrons we used an integral background<sup>19</sup> coupled to the bulk component of the 4*f* emission. Finally, the spectra were convoluted with a Gaussian to simulate the energy dependent spectral resolution of the experimental setup. For each set of data the values of binding energies and spin-orbit splitting (about 1.26 eV) was kept constant. However, variations of the intensity ratio of the 4*f*<sub>5/2</sub> and 4*f*<sub>7/2</sub> components were allowed. The drastic intensity variation of the two components due to the 4*f* core-level cross section limited the working energy range. In particular, the surface component is characterized by a strong decrease of its emission as the photon energy increases. As a result of data evaluation the intensity curves for the 4*f*<sub>7/2</sub> and 4*f*<sub>5/2</sub> com-

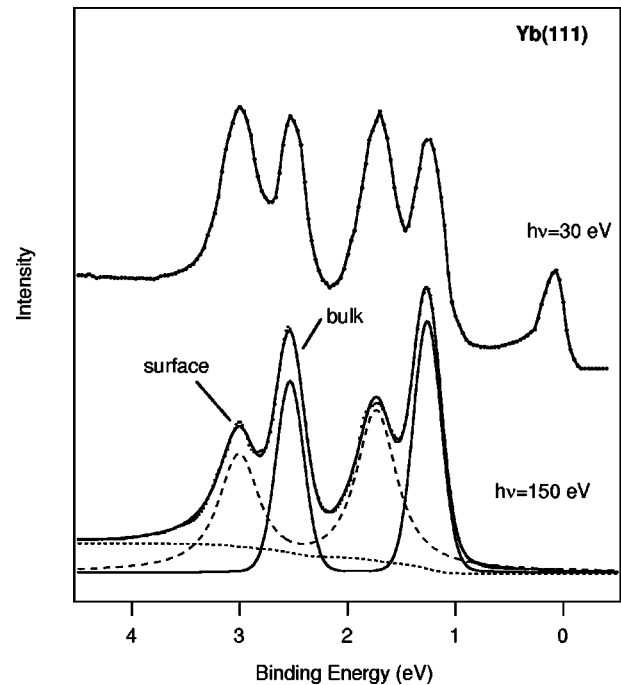


FIG. 1. Yb 4*f* core level PE spectra of Yb(111) single crystalline films obtained at photon energies of 30 and 150 eV (lines through data points). Individual subspectra used to fit the 150 eV spectrum are shown underneath the experimental data.

ponents of both bulk and surface emission were obtained as a function of photon energy and emission angle.

Single scattering simulations were carried out in order to perform a quantitative determination of the surface relaxation. Comparisons between Yb(111) experimental and theoretical curves were estimated by using trial-and-error method. The quality of the agreement was evaluated by the calculation of reliability factors (*R* factor).<sup>20</sup>

The Fig. 2 shows the experimental bulk and surface components Yb 4*f* curves (dotted line), used in the data analysis together with the theoretical (broken line) ones obtained for the *R*-factor minimum. The epitaxial growth mode of Yb thick layer was determined from energy and polar bulk PED curves. The films present a fcc structure with a bulk lattice constant (see Fig. 3) of  $5.44 \pm 0.05$  Å, perfectly in agreement with the tabulated value. Strong intensity modulations of the bulk and surface components were observed at certain detection geometries in which emitter, scatter, and detector were aligned. The surface lattice relaxation determination was based on the surface PED curves. Variation of the interlayer spacing for the two upper surface layers respect to the bulk corresponding value was considered. Difference values between  $-0.4$  and  $0.2$  Å, every 0.03 Å were calculated, i.e., inward or outward relaxations of the last two surface layers (as seen in Fig. 3,  $d_{12}$  represent the interlayer distance top to second layer and  $d_{23}$ , second to third layer, respectively).

A representative contour map of the *R* factor as a function of the parameters  $d_{12}$  and  $d_{23}$  is shown in Fig. 4. This contour tests the sensitivity of the experimental data to the surface layer relaxation respect to the bulk. The shape of the contour implies no correlation of the two parameters, i.e., an increment of the *R* factor produced by a vertical displacement of  $d_{12}$  is not compensated by a movement of  $d_{23}$ . Mini-

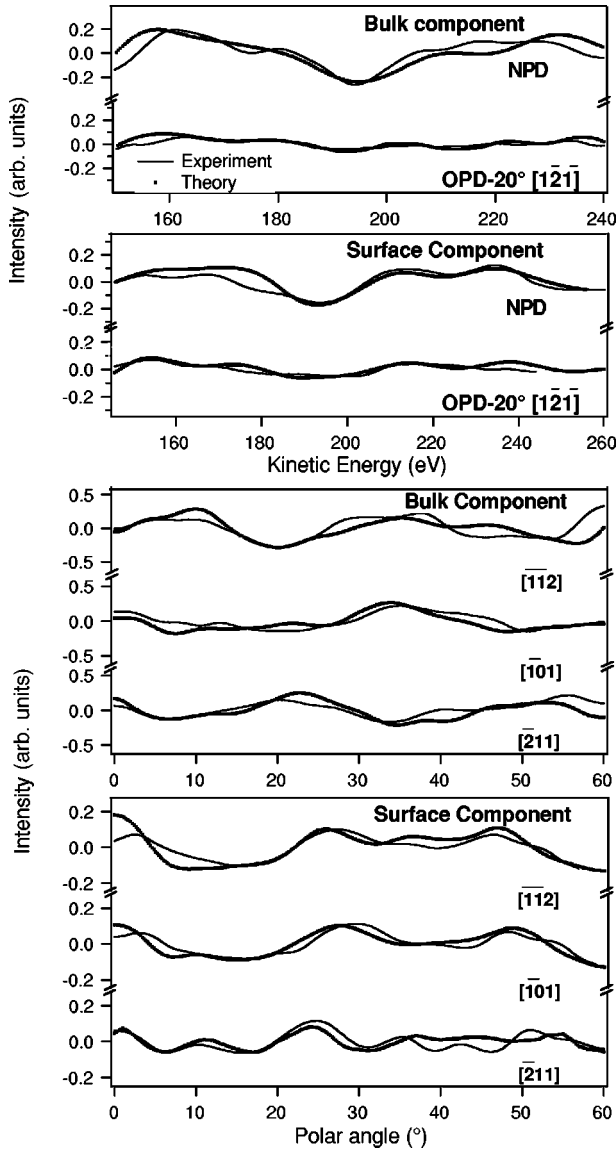


FIG. 2. Comparison of surface and bulk  $4f_{7/2}$  PED patterns from Yb(111) single crystalline films. All intensity values were normalized to photon flux. In the case of energy scans measured in normal emission (NPD) and  $20^\circ$  off-normal emission (OPD- $20^\circ$ ) geometries, the obtained intensities were also normalized to the atomic  $4f$  photoionization cross sections. For angular scans a  $\cos^2(\phi)$  dependence of the photoemission intensity, where the angle  $\phi$  is formed by the electric-field vector of the linearly polarized synchrotron radiation and the direction of the electron detection, was assumed.

imum  $R$  factor is obtained for a difference value of  $\Delta d_{12} = -0.16 \pm 0.01 \text{ \AA}$  and  $\Delta d_{23} = -0.066 \pm 0.005 \text{ \AA}$ , for the first ( $d_{12}$ ) and second ( $d_{23}$ ) surface layers respectively, indicating an inward lattice relaxation in both cases, which correspond to a  $(3.6 \pm 0.3)\%$  and  $(1.9 \pm 0.2)\%$  contraction respect to the bulk interlayer spacing.

Surface lattice relaxations may be caused by different mechanisms. Outward relaxations are usually explained in terms of (1) an enhancement of surface magnetic polarization, (2) minimization of the exchange correlation energy at the surface, or (3) dehybridization. While the first mechanism may be disregarded for divalent  $s$ -band metals, the lat-

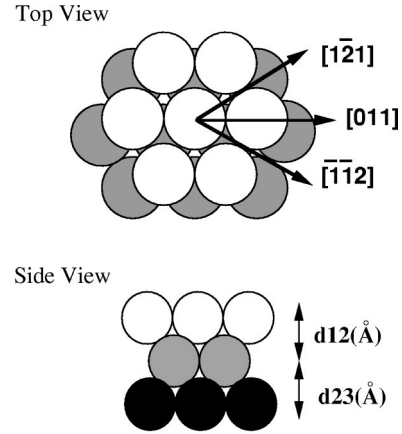


FIG. 3. Top and side views of Yb(111) of a bcc crystal. Crystal directions and coordinate axes are shown.  $d_{12}$  represents the inter-layer distance from the top to the second layer and  $d_{23}$ , from the second to the third layer, respectively.

ter two mechanisms are assumed to be responsible for the outward relaxation of the outermost atomic layers in Be and Mg, where particularly a dehybridization of  $s$  and  $p$  bands leads to decrease of bonding. Inward relaxations will mainly be caused by two mechanisms: (i) variations of electron density by the electron spill-out at the surface and (ii) enhancement of bonding strength by rehybridization of dangling bonds. The first mechanism developed within the framework of a jellium model has been widely applied to discuss surface relaxations in alkali metals and is particularly effective for low coordinated surfaces.<sup>21–23</sup> Minimization of the mean electron kinetic-energy leads here to a smoothing of the electron density contours and thereby, to the formation of an enhanced surface dipole layer. Due to this dipole layer, the positive ion cores feel a net repulsion from the resulting charge in their Wigner-Seitz cells, and an inward relaxation of the outermost atomic surface layer occurs. The relaxation effect, however, becomes rather small at close-packed surfaces. For Na metal (bcc) the inward relaxation at the (100)

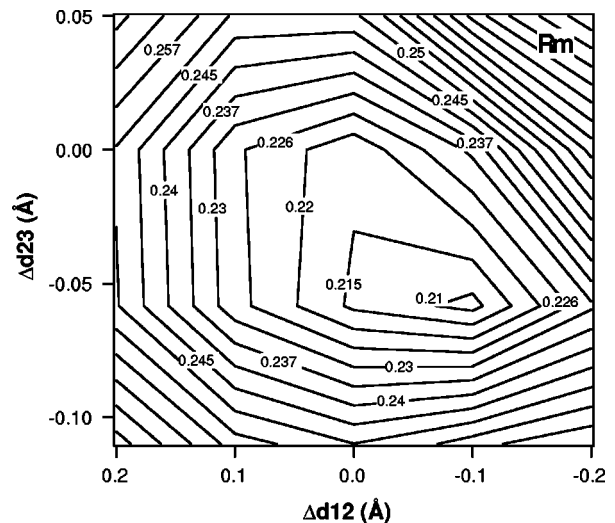


FIG. 4.  $R$ -factor contour plot calculated varying the Yb interlayer spacings  $d_{12}$  and  $d_{23}$ . Best agreement is obtained for inward relaxation differences of  $\Delta d_{12} = -0.1 \text{ \AA}$ , and  $\Delta d_{23} = -0.06 \text{ \AA}$  relative to the bulk interlayer spacing.

surface amounts to only 1% of the lattice constant, and for the close-packed (111) surfaces of a fcc crystals even smaller values are expected, which may easily be compensated by other effects. For example, the Al(111) surface reveals a weak outward relaxation of the outermost atomic surface layer instead of the expected lattice contraction that may be caused by a compensation of the dipole contribution by a *sp* dehybridization effect like in Be and Mg.

In the present case of Yb metal, the *sp* hybridization is widely replaced by *sd* hybridization, but similar to the *sp* metals a dehybridization effect may be expected by narrowing of the *5d* bands. In contrast to the *sp* metals, however, dehybridization at the Yb(111) surface leads to a formation of a *d*-like surface state, which becomes partly occupied around the  $\bar{\Gamma}$  point of the surface Brillouin zone.<sup>14</sup> The charge density distribution related with such a surface state may cause an enhancement of the effective electronic spill out and may be responsible for the inward relaxation observed in the present work. On the other hand, changes of the surface dipole layer should directly affect the work function, and here slab calculation, which do not reproduce the occupied surface state, are in reasonable agreement with experiment. The modulation of the surface dipole layer by the presence of the surface state seems to be small, and it is questionable whether weak variations of the surface dipole will be reflected in the surface relaxation. The second mechanism is characteristic for covalent bonding and, e.g., responsible for the large inward relaxations observed in transition metals that are typically in the range of 3–5 % of the lattice constant. According to our calculations for bulk Yb metal, the *5d* admixtures to the occupied density of states amount to only 0.27 electrons per Yb atom and contribute only weakly to bonding. At the surface, the *d* occupation is enhanced due to the presence of the surface state. According to the slab calculation, however, this state is not explicitly present at the (111) surface of divalent Yb metal and is non-

bonding at the close-packed surfaces of trivalent RE metals. At the same time, the model calculations predict this state to be unoccupied in the paramagnetic phase, what is obviously in disagreement with experiment. An energetically lowering of this surface state may be achieved either by participation in bonding or by reducing the electron kinetic energy by delocalization. Both effects will support inward relaxation, the first due to enhanced surface bonding via mechanism (ii), the second due to increased electronic spill-out via mechanism (i).

In summary, we have shown by a PED experiment, that the outermost atomic layers for *in situ* Yb(111) grown single-crystals are subject to an inward bulk interlayer relaxation that amounts ( $3.66 \pm 0.3$ )% for the first and ( $1.9 \pm 0.2$ )% for the second layer. This behavior deviates considerably from the one of the divalent metals Be and Mg, which are characterized by outward relaxations. The main difference between these systems is the appearance of a *d*-like surface state at Yb(111), which consequently is assumed to be responsible for the inward relaxation at this surface. This finding may have important consequences for the lattice relaxations of trivalent RE's, where also inward relaxations may be expected in contrast to the theoretically predicted outward relaxations. Variations of the surface lattice constants, however, will affect the magnetic properties and might be responsible for the ferromagnetic coupling of the outermost surface layer of Gd(0001) and the enhanced magnetic ordering temperature observed for Gd and other RE metals.<sup>6,9</sup>

This work has been supported by the Spanish agency DGES under Grant No. PB-97-1199, the Comunidad de Madrid (Grant No. 07N/0031/1998) and the Deutsche Forschungsgemeinschaft, Sonderforschungsbereich 463, TP B4. M.E.D. acknowledges financial support from the Comunidad de Madrid.

- 
- <sup>1</sup>S. P. Chen, Surf. Sci. Lett. **264**, L162 (1992).  
<sup>2</sup>R. Wu *et al.*, Phys. Rev. B **44**, 9400 (1991).  
<sup>3</sup>A. Stenborg *et al.*, Phys. Rev. Lett. **63**, 187 (1989).  
<sup>4</sup>C. Walfried *et al.*, Phys. Rev. B **48**, 7434 (1998).  
<sup>5</sup>M. Getzlaff *et al.*, J. Magn. Magn. Mater. **184**, 155 (1998).  
<sup>6</sup>D. Weller *et al.*, Phys. Rev. Lett. **54**, 1555 (1985).  
<sup>7</sup>C. Rau *et al.*, Phys. Rev. B **34**, 6347 (1986).  
<sup>8</sup>B. Kim *et al.*, Phys. Rev. Lett. **68**, 1931 (1992).  
<sup>9</sup>G. A. Mulhollan *et al.*, Phys. Rev. Lett. **69**, 3240 (1992).  
<sup>10</sup>A. V. Fedorov *et al.*, Phys. Rev. B **50**, 2739 (1994).  
<sup>11</sup>S. C. Wu *et al.*, Phys. Rev. B **45**, 8867 (1992).  
<sup>12</sup>A. V. Fedorov *et al.*, Phys. Rev. B **49**, 5117 (1994).  
<sup>13</sup>G. Kaindl *et al.*, Phys. Rev. B **51**, 7920 (1995).  
<sup>14</sup>M. Bodenbach *et al.*, Phys. Rev. B **50**, 14 446 (1994).  
<sup>15</sup>E. Navas *et al.*, Phys. Rev. B **48**, 14 753 (1993).  
<sup>16</sup>A. F. Wright *et al.*, Surf. Sci. **302**, 215 (1994).  
<sup>17</sup>P. J. Feibelman, Phys. Rev. B **49**, 13 809 (1994).  
<sup>18</sup>P. J. Feibelman *et al.*, Phys. Rev. B **50**, 17 480 (1994).  
<sup>19</sup>A. Shirley, Phys. Rev. B **5**, 4709 (1972).  
<sup>20</sup>K. M. Schindler *et al.*, Phys. Rev. B **46**, 4836 (1992).  
<sup>21</sup>K.-P. Bohnen, Surf. Sci. **147**, 304 (1984).  
<sup>22</sup>P. Blaise *et al.*, Surf. Sci. **221**, 513 (1989).  
<sup>23</sup>P. Jiang *et al.*, Solid State Commun. **59**, 275 (1986).